ELSEVIER

International Journal of Mass Spectrometry and Ion Processes 171 (1997) 83–93

International Journal of Mass Spectrometry and Ion Processes

Dissociative ionization of silane by electron impact

R. Basner[a], M. Schmidt[a,*], V. Tarnovsky[b], K. Becker[1,b], H. Deutsch[c]

[a]*Institut für Niedertemperatur-Plasmaphysik, Robert-Blum-Str. 8–10, 17489 Greifswald, Germany*
[b]*Physics Department, City College of C.U.N.Y., New York, NY 10031, USA*
[c]*Ernst-Moritz-Arndt-Universität, Fachrichtung Physik, Domstr. 10a, 17489 Greifswald, Germany*

Received 3 March 1997; accepted 7 May 1997

Abstract

We studied the electron impact ionization of silane (SiH_4) which is widely used in the plasma deposition of different silicon-containing thin films. Absolute partial cross-sections for the formation of all fragment ions were measured in a high resolution double focusing sector field mass spectrometer with a modified ion extraction stage for electron energies from threshold to 100 eV. No evidence for the formation of stable parent SiH_4^+ ions was found in agreement with previous experimental investigations. The single positive fragment ion formation is the dominant ionization process. We observed the following product ions: SiH_3^+, SiH_2^+, SiH^+, Si^+, H_2^+, and H^+. The agreement between our measured absolute partial ionization cross-sections and two earlier data sets obtained by different techniques is generally good for the silicon-containing fragment ions taking into account quoted uncertainties of ± 10% to ± 20%, but less satisfactory for the formation of atomic and molecular hydrogen ions which were found to be produced with significant excess kinetic energies, particularly in the case of H^+. A comparison of the total SiH_4 ionization cross-section derived from the measured partial ionization cross-sections and a calculated cross-section based on the Binary-Encounter-Bethe (BEB) model showed excellent agreement in the energy range above 30 eV. © 1997 Elsevier Science B.V.

Keywords: Cross-sections; Electron impact ionization; Plasma processing

PACS classification: 34.80Gs; 52.20Fs

1. Introduction

The plasma-assisted deposition of thin films for surface protection, optics, electronics and biomedicine is a rapidly growing field in plasma technology. Amorphous silicon [1–4], silicon nitride [5], SiO_2 [6] and (Ti,Si)N [7] are produced by plasma-assisted chemical vapor deposition using silane (SiH_4) as the precursor of choice. Complete sets of electron collision cross-sections for SiH_4 are needed for the modeling of silane-containing plasmas [8–10]. Total and partial electron-impact ionization cross-sections for SiH_4 are important for the understanding and modeling of the charge carrier balance in the plasma and the ion/radical chemistry in the gas phase as well as for the surface processes [11]. Photoabsorption and photoionization cross-sections [12–14] and the electron-impact ionization of silane and its

* Corresponding author.
[1] Present Address: Department of Physics and Engineering Physics, Stevens Institute of Technology, Hoboken, NJ 07030, USA.

PII S0168-1176(97)00063-3

radicals [15–18] have already been studied by several groups. Absolute partial SiH_4 ionization cross-sections were reported by Chatham et al. [15] and by Krishnakumar and Srivastava [16] using quadrupole mass spectrometric methods. Haaland [17] estimated the cross-sections for the formation of SiH_3^+, SiH_2^+, SiH^+ and Si^+ by scaling the published values of Chatham et al. [15] and the differential data of Morrison and Traeger [19] to his absolute cross-section values at 50 eV which were obtained with a Fourier transform mass spectrometer. The resulting cross-sections of Haaland [17] are lower by a factor of two to three compared to the data of Chatham et al. [15] and Krishnakumar and Srivastava [16]. In contrast to Chatham et al. [15] and Krishnakumar and Srivastava [16] (and the present results, see below), Haaland [17] did not find any evidence of H^+ and H_2^+ fragment ions. The cross-sections reported by Chatham et al. [15] and by Krishnakumar and Srivastava [16] show differences in the absolute values of about 30% for SiH_3^+ and less for other fragment ions with the exception of H_2^+ and H^+, where Chatham et al. [15] only report measurements at a few selected energies (30 eV, 50 eV, and 100 eV) and relied on the low energy data from Morrison and Traeger [19]. Krishnakumar and Srivastava [16], on the other hand, reported complete cross-section data from threshold up to 1000 eV for all fragment ions. Their cross-section shapes for SiH_2^+, SiH^+, Si^+, and H_2^+ show pronounced maxima at very low energies between 25 eV and 40 eV and decline monotonically toward higher impact energies. Their total ionization cross-section reaches its maximum slightly below 50 eV. By contrast, the cross-section shapes reported by Chatham et al. [15] peak at higher energies around 60 eV.

In this paper we report the results of silane ionization cross-section measurements carried out using a high resolution double focusing sector field mass spectrometer. A complete set of partial electron-impact ionization cross-sections for the formation of SiH_3^+, SiH_2^+, SiH^+, Si^+, H^+, and H_2^+ was obtained from threshold to 100 eV. The measured partial ionization cross-sections were combined to a total ionization cross-section which is compared with calculated total ionization cross-sections using the Binary-Encounter-Bethe (BEB) model [20] and a modified additivity rule [21].

2. Experimental

The experimental apparatus and the measurement technique employed here have been described in several previous publications [22–25]. A high-resolution ($m/\Delta m$ = 40 000) double focusing sector field mass spectrometer MCH 1310 with a Nier-type electron-impact ion source was used for the measurements. The target gas pressure in the ion source, which is typically in the range 0.1 to 1 mPa compared to a background pressure of 0.001 mPa, was measured with a spinning rotor viscosity gauge. The electron gun was operated with a stabilized electron beam current of 10 μA emitted from a directly heated tungsten band cathode. The impact energy was varied from 5 eV to 100 eV. The energy spread of the electron beam, which is collimated by a weak longitudinal magnetic field of 200 G, was about 0.5 eV (FWHM). The temperature of the ion source was kept at 120°C. The ions were extracted from the ionization region by a penetrating electric field. The acceleration voltage between the ion source and the entrance slit of the mass spectrometer was 5 kV. The ion repeller potential was kept at the potential of the ionization chamber. Argon, which is used as reference gas, was always added to silane for calibration purposes. The ion efficiency curves (relative ionization cross-sections) were measured simultaneously for Ar and SiH_4 in a well-defined mixture in an effort to ensure equal operating conditions for the detection of the SiH_4 fragment ions and the Ar^+ and Ar^{++} ions. The measured relative partial ionization cross-sections were put on an absolute scale by normalization relative

to the total Ar ionization cross-section of 2.77×10^{-16} cm^2 at 70 eV [26].

The reliability of the mass spectrometric technique for the measurement of parent ionization cross-sections and, more recently, also for fragment ionization cross-sections was demonstrated by Märk and co-workers [27–30]. These authors pointed out that discrimination effects and the loss of energetic fragment ions must be accounted for in order to obtain reliable dissociative ionization cross-sections. Earlier measurements of the NF_3 parent and fragment ionization cross-sections in our apparatus [22] revealed a significant loss of energetic fragment ions. As a consequence, the ion optics for the extraction, acceleration and deflection of the ions was rebuilt based on ion trajectory simulations [31] in conjunction with *in situ* experimental studies in an effort to minimize and/or quantify the discrimination of energetic fragment ions. The modified mass spectrometer can now be operated either in a high mass resolution mode (with significant discrimination effects present) or in a high extraction efficiency mode (by partially sacrificing the high mass resolution capability, with a resulting mass resolution of 2000). Fig. 1 shows the ion extraction efficiencies in the two modes of operation as a function of the excess kinetic energy of the fragment ion as obtained from ion trajectory simulations. The curves demonstrate that significant ion losses occur in the high resolution mode for excess energies as low as 0.1 eV and about 50% of all ions are lost for an excess energy of 1 eV per fragment ion. By contrast, there are essentially no ion losses for excess energies of up to 3 eV per fragment ion when the instrument is operated in the high extraction efficiency mode. Recent ionization cross-section measurements for SO_2 [23] carried out in our modified mass spectrometer as well as in a fast-neutral beam apparatus, which is less sensitive to discrimination effects, confirmed experimentally that the mass spectrometer operated in the high extraction efficiency mode can detect energetic fragment ions efficiently as long as the excess kinetic energy is not too large (e.g. less than about 1 eV per fragment in the case of SO^+, S^+, and O^+ from SO_2 [23]). Similar findings were reported recently for the formation of the CH_3^+ fragment ion produced by dissociative ionization of tetramethylsilane, TMS [32]. For all measurements reported here, the data acquisition procedure included a horizontal sweep of the ion beam across the entrance slit of the mass spectrometer and absolute cross-sections were obtained by integrating the ion signal over the ion beam profile (see Fig. 2). We are aware that in general, accurate absolute ionization cross-sections are only obtained, when the ion beam is also deflected vertically along the

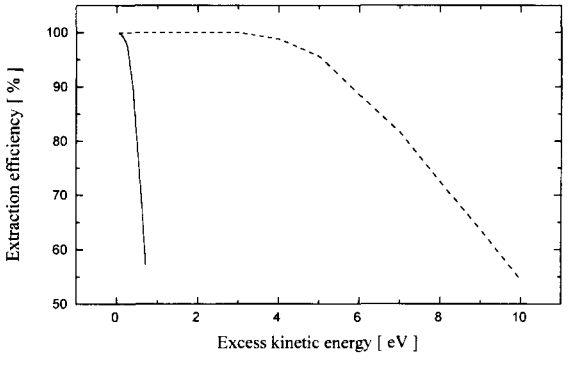

Fig. 1. Calculated ion extraction efficiency of the ion source as a function of excess kinetic energy per fragment ion for the high mass resolution mode (-) and the high extraction efficiency mode (- - -). The calculations use the SIMION ion trajectory modeling code [31].

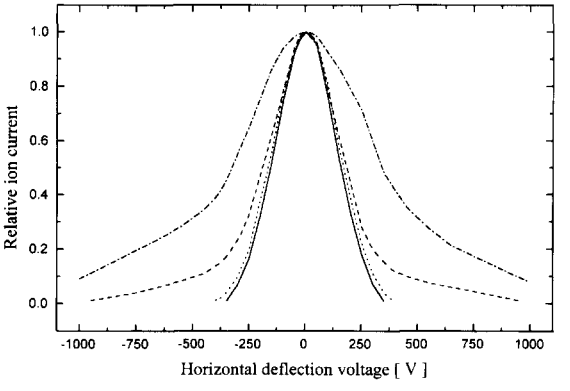

Fig. 2. Normalized ion currents of the extracted H^+ (-···-), H_2^+ (- - -), Si^+ (···), and SiH_3^+ (-) fragment ion beams from silane as a function of the horizontal deflection voltage.

direction of the entrance slit and the beam profile is also integrated in the vertical direction [30]. However, it has been demonstrated that corrections resulting from the vertical integration are small as long as the excess kinetic energy of the fragment ions is small [33]. In the present case, the only fragment ion signal for which a vertical integration could result in an appreciable change is the H^+ signal. As discussed later in detail, we only give a lower limit for that particular partial cross-section in any case.

3. Results and discussion

As a first step, we recorded the mass spectrum of silane at an impact energy of 70 eV with the mass spectrometer operated in the high extraction efficiency mode. The SiH_4 mass spectrum is dominated by singly charged ions. The measured relative intensities (obtained by integration over the ion beam profile, see Fig. 2) of 100%, 81%, 30.1%, 26.4%, 13.3%, 7.4%, 5.6%, and 2.5% for the mass-to-charge (m/z) ratios 30, 31, 29, 28, 1, 32, 2, and 33 agree very well with the cracking pattern from the Eight Peak Index and other data bases [34] with the exception of m/z 1 and 2 which correspond to atomic and molecular hydrogen ions. The Eight Peak Index [34] shows less than 1/4 of our H_2^+ intensity and gives no indication of H^+ ions. In the course of this work, we observed that H_2^+ ions from two sources contribute to our measured H_2^+ ion signal, ions from the dissociative ionization of silane and ions from the direct ionization of H_2 resulting from the pyrolytic decomposition of silane at the hot filament of the electron gun (see discussion below). Doubly charged ions were detected at m/z 14, 14.5, 15 and 15.5, but with very low intensities of 0.3%, 0.9%, 0.6% and 0.06% of the most abundant ion signal at m/z 30. The ion signal at m/z 30 consists of contributions from 0.8% $^{30}Si^+$, 1.3% $^{29}SiH^+$ and 97.9% $^{28}SiH_2^+$. We note that the ratios of the relative intensities of the doubly charged ions are very different compared to the corresponding ratios for the singly charged ions.

Measurements of the ion efficiency curves with special emphasis on the near-threshold region were carried out next in order to determine the appearance energy of each fragment ion. Our results measured in the high extraction efficiency mode of 12.2 ± 0.5 eV (SiH_3^+), 11.6 ± 0.6 eV (SiH_2^+), 15.1 ± 0.5 eV (SiH^+), 13.6 ± 0.5 eV (Si^+), 24.3 ± 1.0 eV (H_2^+), and 24.5 ± 0.6 eV (H^+) agree very well with previously determined values summarized in Ref. [16]. The measured appearance energies for H^+ and H_2^+ are supported by the earlier (e, 2e) scattering experiments of Cooper et al. [35] who reported dissociative photoionization thresholds near 24.5 eV for both H^+ and H_2^+. The quoted uncertainties in our measured value are due to the inherent energy spread of the electron beam and a small residual electric field in the interaction region from the penetrating ion extraction field which causes some extended curvature in the near-threshold region. We observed a slightly more extended curvature for the silane fragment ions compared to the rare gases Ar, Kr and Xe which were used for calibrating the electron energy scale. We attribute this to the presence of different ionization channels with different appearance energies at a given m/z value, e.g. ion signals arising from ions containing different Si isotopes such as m/z 30 (see above).

Natural Si is dominated by a single isotope, ^{28}Si with an abundance of 92.3%. Other isotopes are much less abundant, ^{29}Si (4.7%) and ^{30}Si (3.0%). As a consequence, the contamination of the recorded ion signals due to isotope effects is small compared to the overall uncertainty (±18%) of the measured absolute ionization cross-sections. Nevertheless, we corrected the shape and the absolute values of each measured ion efficiency curve for these isotope effects. We started with m/z 28 which contains only contributions from $^{28}Si^+$. From that we calculated the contribution of $^{29}Si^+$ to the measured signal at m/z 29 and after subtraction we obtain

the pure signal attributable to $^{28}SiH^+$. Cross-sections for the isotopically pure fragment ions $^{28}SiH_2^+$ and $^{28}SiH_3^+$ were obtained in a similar fashion. The partial cross-section for every silicon-containing fragment ion was then obtained by adding the various isotope contributions. We also note that the mass resolution of the mass spectrometer in the high extraction efficiency mode is high enough to separate the small ion signal arising from background nitrogen from that of $^{28}Si^+$.

3.1. The formation of Si-containing fragment ions

As mentioned before, we found no detectable parent SiH_4^+ ion signal. This is the result of the instability of SiH_4^+ and its decay into SiH_2^+ and H_2. The values of all six measured partial ionization cross-sections (SiH_3^+, SiH_2^+, SiH^+, Si^+, H_2^+, and H^+) averaged over several independent data runs are given in Table 1. Also given is the absolute total single ionization cross-section which was obtained as the sum of the partial ionization cross-sections. Dissociative ionization of the parent silane molecule is the only source of the observed silicon-containing fragment ions. The measured appearance energies indicate that the direct ionization of radicals [18] formed in the ion source does not contribute to the detected ion signals.

Fig. 3 shows our partial ionization cross-sections for SiH_3^+ and SiH_2^+ in the energy region

Table 1
Absolute partial ionization cross-sections for the formation of SiH_3^+, SiH_2^+, SiH^+, Si^+, H_2^+, and H^+ fragment ions by electron impact on SiH_4. Also given is the absolute total SiH_4 single ionization cross-section

Electron energy (eV)	Ionization cross-section (10^{-16} cm^2)						
	Ion						
	H^+	H_2^+	Si^+	SiH^+	SiH_2^+	SiH_3^+	Total
12					0.06		0.06
13					0.15	0.07	0.22
14			0.01		0.31	0.20	0.52
15			0.03		0.55	0.36	0.94
16			0.04	0.02	0.86	0.57	1.49
17			0.05	0.03	1.09	0.81	1.98
18			0.06	0.07	1.35	0.96	2.44
19			0.08	0.12	1.58	1.11	2.89
20			0.10	0.18	1.69	1.22	3.19
22			0.14	0.28	1.87	1.36	3.65
24			0.19	0.41	1.93	1.40	3.93
26	0.02	0.003	0.27	0.51	1.97	1.41	4.18
28	0.06	0.005	0.33	0.55	2.00	1.44	4.39
30	0.08	0.007	0.39	0.57	2.03	1.46	4.54
32	0.13	0.009	0.43	0.59	2.06	1.48	4.70
34	0.17	0.011	0.47	0.61	2.07	1.49	4.81
36	0.19	0.014	0.49	0.61	2.08	1.51	4.89
38	0.22	0.017	0.51	0.62	2.09	1.51	4.97
40	0.24	0.020	0.52	0.62	2.09	1.52	5.01
45	0.27	0.024	0.54	0.64	2.08	1.54	5.09
50	0.28	0.028	0.56	0.65	2.11	1.56	5.19
55	0.28	0.031	0.58	0.65	2.14	1.59	5.27
60	0.28	0.033	0.58	0.65	2.16	1.61	5.31
70	0.28	0.035	0.59	0.64	2.18	1.67	5.40
80	0.28	0.035	0.59	0.63	2.14	1.66	5.34
90	0.27	0.035	0.57	0.60	2.08	1.63	5.19
100	0.27	0.035	0.55	0.58	2.05	1.59	5.08

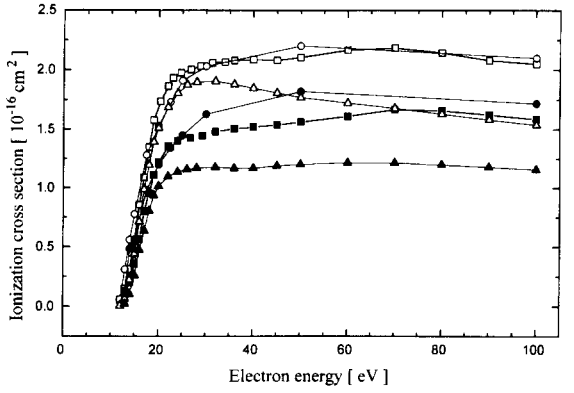

Fig. 3. Absolute partial SiH_3^+ (filled symbols: ■, ●, ▲) and SiH_2^+ (open symbols: □, ○, △) ionization cross-sections as a function of electron energy. The squares (■,□) represent the present results. Also shown are the previous cross sections of Chatham et al. (●,○) and Krishnakmar and Srivastava (▲,△).

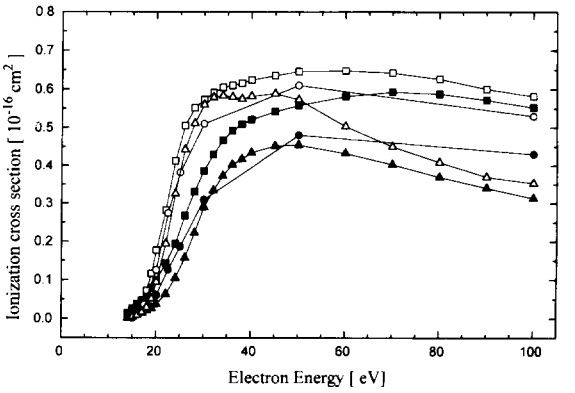

Fig. 4. Same as Fig. 3 for the formation of Si^+ (filled symbols: ■, ●, ▲) and SiH^+ (open symbols: □, ○, △) fragment ions.

from threshold to 100 eV together with the earlier results of Chatham et al. [15] and Krishnakumar and Srivastava [16] in the same energy region. Our measurements were carried out at 0.2 eV energy intervals. There is excellent agreement between our cross-sections and the data of Chatham et al. [15] both in terms of the absolute cross-section values and the cross-section shapes (less than 10% difference for energies above 20 eV). The SiH_3^+ cross-section of Krishnakumar and Srivastava [16] is lower than our value by about 25%, but there is good agreement in the cross-section shapes. For SiH_2^+, on the other hand, the cross-section curve of Krishnakumar and Srivastava [16] declines much more rapidly than our cross-section for impact energies above about 20 eV. At 100 eV, their absolute cross-section is about 30% below our value. We note that our cross-section values did not change whether the mass spectrometer was operated in the high resolution mode or in the high extraction efficiency mode. Moreover, the measured ion beam profiles for SiH_3^+ (see Fig. 2) and SiH_2^+ were identical to the Ar^+ ion beam profile. This finding indicates that these fragment ions are formed with little, if any, excess kinetic energy [36,37].

The same procedure was applied to the measurement of the SiH^+ and Si^+ fragment ions. The identical ion beam profiles in these cases showed a slight broadening (see Fig. 2 for Si^+) indicating that the ions are formed with a small amount of excess kinetic energy, which was however not sufficient to cause any significant ion loss as long as the mass spectrometer was operated in the high extraction efficiency mode. There is no information in the literature regarding the excess kinetic energy of Si^+ and SiH^+ ions formed by dissociative ionization of SiH_4. Perrin and Aarts [38] reported translational energies of about 0.07 eV for the formation of ground state SiH fragment produced by 40–70 eV electron impact on silane and argued that most fragments should have small translational energies in the order of 0.1 eV. Fig. 4 shows the SiH^+ and Si^+ cross-sections obtained in this work again in comparison with the earlier data of Chatham et al. [15] and Krishnakumar and Srivastava [16]. As before, there is good agreement between our SiH^+ data and those of Chatham et al. [15]. Our data appear to be consistently higher by about 10% which is well within the combined error margins of both measurements. The corresponding cross-section of Krishnakumar and Srivastava [16] is different in shape, again declining much faster toward higher impact energies and displaying a pronounced double-peak in the 25–40 eV energy

region, which none of the other measurements shows. In the case of the Si^+ cross-section, our measured data lie above the data reported by both Chatham et al. [15] and Krishnakumar and Srivastava [16], but the different data agree within their combined margin of error.

3.2. The formation of atomic and molecular hydrogen fragment ions

The previous studies of the electron-impact ionization of SiH_4 revealed differences in the H_2^+ partial ionization cross-sections in terms of absolute cross-section value and energy dependence. We carried out extensive studies of the ion beam profiles of both the H_2^+ and H^+ ions. Fig. 2 shows the measured H_2^+ and H^+ ion beam profiles together with the profiles of the SiH_3^+ and Si^+ fragment ions. We note that the SiH_3^+ and Si^+ beam profiles are essentially identical to the profile obtained for the Ar^+ ions, which are formed with no excess kinetic energy, whereas the H_2^+ and H^+ ion beam profiles show a considerable broadening caused by excess kinetic energy. In Fig. 5 we present several measured H_2^+ ionization cross-sections, a H_2^+ cross-section from H_2 measured in our apparatus, the 'benchmark' H_2 total ionization cross-section of Rapp and Englander-Golden [26], and two H_2^+ cross-sections from SiH_4 measured in our apparatus for two different ion beam deflection voltages, 0 V (which corresponds to the center of the H_2^+ ion beam profile) and 400 V (which corresponds to the wing of the H_2^+ ion beam profile). The various relative cross-section measurements were normalized to one another at 70 eV. There is essentially perfect agreement between the two cross-section curves for H_2^+ from H_2 and the H_2^+ cross-section from SiH_4 obtained at 0 V deflection voltage. All three H_2^+ cross-section curves show appearance energies consistent with the 15.426 eV ionization energy of H_2 [39]. Extensive experimental checks ruled out background, multiple collisions, or impurities of any kind as a possible source for the H_2^+ signal from SiH_4 in our measurements. We attribute the H_2^+ from silane to the ionization of H_2 produced by the pyrolytic decomposition of silane at the hot electron gun filament. Thermal decomposition of silane is known to start at temperatures as low as 300°C [40]. The cross-section shape and appearance energy of the H_2^+ ions change little as we increase the ion beam deflection voltage (and thus probe the wings of the H_2^+ ion signal) until we reach deflection voltages above about 300 V and begin to detect ions in the far wing of the H_2^+ ion beam profile. The H_2^+ ionization cross-section curve recorded at a deflection of 400 V, the fourth curve shown in Fig. 5, is distinctly different from the other three curves, most notably the appearance energy has shifted to 24.3 ± 1.0 eV, which is in good agreement with the H_2^+ appearance energy reported by Krishnakumar and Srivastava [16]. We interpret these observations in the following way:

(i) H_2^+ ions are formed via at least two processes in our ion source, the direct ionization of H_2 resulting from the pyrolytic decomposition of SiH_4 at the hot filament (characterized by an appearance energy of 15.4 eV) and the dissociative ionization of SiH_4 (characterized by an appearance energy of 24.5 eV).

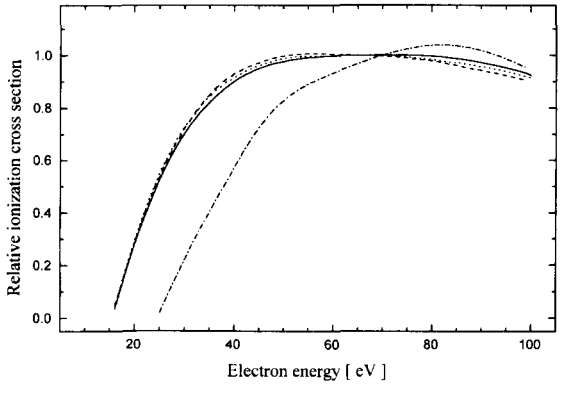

Fig. 5. Relative total H_2 ionization cross-section of Rapp and Englander-Golden [26] (-) in comparison with the measured relative partial H_2^+ ionization cross-sections from H_2 (deflection voltage 0 V: (···) and SiH_4 (deflection voltages 0 V: (- - -) and 400 V: (-·-·-) as a function of electron energy. (See text for further details.)

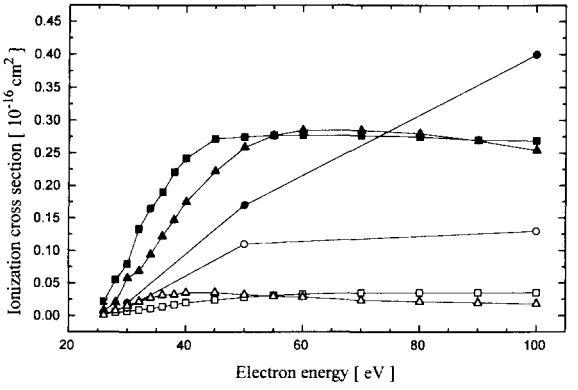

Fig. 6. Same as Fig. 3 for the formation of H^+ (filled symbols: ■, ●, ▲) and H_2^+ (open symbols: □, ○, △) fragment ions.

(ii) Most H_2^+ ions resulting from the dissociative ionization of SiH_4 are formed with excess kinetic energy as evidenced by their absence from the H_2^+ ionization cross-section curve recorded at zero and low deflection voltages—we found no evidence of a change in the slope of the H_2^+ cross-section curves around 24.5 eV obtained at low deflection voltage conditions.

(iii) The H_2^+ ions formed via the direct ionization of H_2 resulting from the pyrolytical decomposition of silane are produced with no excess kinetic energy. This is evidenced by the absence of H_2^+ ions from H_2 in the H_2^+ ion signals obtained at high deflection voltages.

(iv) An attempt was made to deconvolute the two contributions to the total H_2^+ ions signal. The fraction of H_2^+ ions from silane was determined from the ratio of the normalized integrated H_2^+ ion beam intensity from H_2 to that from SiH_4. We estimate that about 1/3 of all recorded H_2^+ ions are 'hot' H_2^+ ions from silane. This estimate represents a lower limit, since there is the possibility that a small fraction of H_2^+ ions from silane are formed with little or no excess kinetic energy. Fig. 6 shows our measured H_2^+ and H^+ partial ionization cross-sections together with similar data reported earlier by Chatham et al. [15] and by Krishnakumar and Srivastava [16]. Our H_2^+ cross-section agrees reasonably well with the cross-section of Krishnakumar and Srivastava [16], whereas Chatham et al. [15] reported H_2^+ cross-sections which were significantly larger.

The measured appearance energy for H^+ ions indicated that the recorded H^+ ion signal was not affected by the presence of H^+ ions resulting from the ionization of H atoms produced by the pyrolysis of SiH_4. The broad H^+ ion beam profile is evidence of the fact that the H^+ fragment ions are formed with a wide distribution of excess kinetic energies (see Fig. 2). The H^+ beam profile from SiH_4 is very similar to the beam profile of H^+ ions produced by dissociative ionization of H_2 which are known to have a broad excess kinetic energy distribution peaking at about 8 eV [41,42]. The dissociation of SiH_4 into 'hot' excited H atoms with translational energies of a few electronvolts was studied by analyzing the Doppler broadening of the subsequently emitted Lyman [43] and Balmer [38,44] lines. The largest deflection voltage used in the present experiment (1000 V) was not high enough to achieve complete collection of all H^+ ions. We determined the absolute H^+ ionization cross-section by extrapolating the measured H^+ beam profile to zero intensity and integrated over the extrapolated ion beam profile. Since we cannot exclude additional losses of energetic H^+ ions (e.g. incomplete extraction from the ion source), our reported H^+ partial ionization cross-section represent only a lower limit. Our H^+ cross-section is in good agreement with the cross-section reported by Krishnakumar and Srivasta [16] except for a slight discrepancy in the cross-section shape in the low energy region below 40 eV. As before for H_2^+, the H^+ cross-section of Chatham et al. [15] is in poor agreement with the other two results.

3.3. The total single ionization cross-section of silane

The total single ionization cross-section of silane was derived by adding the measured partial ionization cross-sections (tabulated values of the total cross-section are given in the last column of Table 1). Total ionization cross-sections

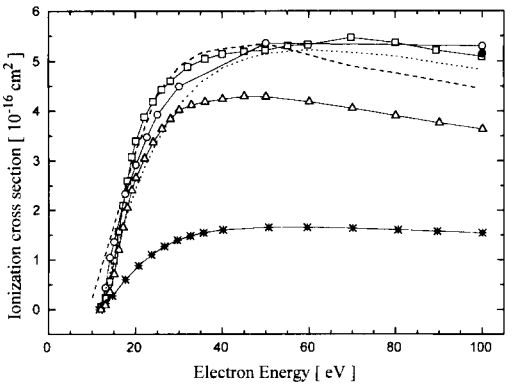

Fig. 7. Absolute total single SiH_4 ionization cross-sections as a function of electron energy: (□) the present results, (○) the previous cross-section of Chatham et al. and (△) Krishnakumar and Srivastava. Also shown are the measured cross-section of Haaland [17] (*), calculated cross-sections using the BEB method [46] (···) and the modified additivity rule (- - -) and the experimental total cross-section of Perrin et al. [45] at a single electron energy of 100 eV (●).

were also reported by Chatham et al. [15], who measured the total SiH_4 ionization cross-sections directly, and by Krishnakumar and Srivastava [16] and by Haaland [17], who obtained their cross-sections in a fashion similar to ours. Fig. 7 shows our total single silane ionization cross-section in comparison with the other three reported cross-sections for impact energies up to 100 eV. Also shown is the measured total SiH_4 ionzation cross-section reported by Perrin et al. [45] at a single impact energy of 100 eV. In addition, we included the result of a BEB calculation by Kim and collaborators [20,46] and our calculated cross-section using a modified additivity rule [21]. There is excellent agreement between our experimentally determined cross-section, the experimental cross-section of Chatham et al. [15], the single data point reported by Perrin et al. [45], the calculated BEB cross-section [46] and our result of calculation. The cross-section reported by Krishnakumar and Srivastava [16] agrees with the other data up to an energy of about 30 eV, but declines more rapidly toward higher impact energies. At 100 eV, their total cross-section is about 30% lower than ours. The total cross-section reported by Haaland is even smaller and lies well outside the combined error margins of all other measurements and the calculations.

4. Summary and conclusions

We measured absolute partial cross-sections for the electron impact ionization of silane, SiH_4, using a modified high-resolution double-focusing sector field mass spectrometer. Dissociative ionization channels are the dominant ion formation processes. Excellent agreement was found between our measurements and the earlier results of Chatham et al. [15] for all Si-containing fragment ions, whereas there are some discrepancies (at the 20–30% level) between our data and the results of Krishnakumar and Srivastava [16], particularly for impact energies above about 25 eV. The cross-sections reported by Haaland [17] using Fourier transform mass spectrometry appear to be consistently smaller than all other measured cross-sections by a factor of two to three. The Si-containing fragment ions appear to be formed with no or only little excess kinetic energy. By contrast, we found that H^+ fragment ions from silane are formed with a broad distribution of excess kinetic energies peaking at several eV per fragment. Our estimated H^+ cross-section agrees very well with the earlier H^+ data of Krishnakumar and Srivastava [16]. The formation of H_2^+ fragment ions measured in our experiment came from two sources, the direct ionization of H_2 produced by the pyrolytic decomposition of SiH_4 at the hot filament of our electron gun and by the dissociative ionization of the parent SiH_4 molecule. Our estimated dissociative H_2^+ ionization cross-section again agrees very well with the earlier H_2^+ cross-section of Krishnakumar and Srivastava [16]. The partial ionization cross-sections were combined to yield the total single SiH_4 ionization cross-section. Our experimental result is in excellent agreement with the earlier experimental results of Chatham et al. [15] and Perrin et al. [45] and with both

calculations, the BEB calculation of Kim and coworkers [46] and our modified additivity rule calculation. The total cross-section reported by Krishnakumar and Srivastava [16] agrees with our data up to an energy of 25 eV, but declines more rapidly toward higher impact energies. The cross-section derived by Haaland [17] lies significantly below all other total ionization cross-section functions.

Acknowledgements

The authors are grateful for the technical assistance provided by Ms. U. Haeder. Two of us (VT, KB) would like to acknowledge partial support of this work by the Division of Chemical Sciences, Office of Basic Energy Sciences, Office of Energy Research, U.S. Department of Energy. We are grateful for travel support from a NATO Collaborative Research Grant (CRG-920089) and from the INP Greifswald. We would like to thank Dr. Y.-K. Kim for making the results of his calculations available to us prior to publication. KB and VT would like to thank their collaborators and the INP Greifswald for their hospitality and support during several visits.

References

[1] J.R. Doyle, D.A. Dougthy, A. Gallagher, J. Appl. Phys. 68 (1990) 4375.
[2] F. Tochikubo, A. Suzuki, S. Kakuta, Y. Terazono, T. Makabe, J. Appl. Phys. 68 (1990) 5532.
[3] G. Turban, Y. Catherine, B. Grolleau, Thin Solid Films 67 (1980) 309.
[4] R. Robertson, D. Hils, H. Chatham, A. Gallagher, Appl. Phys. Lett. 43 (1983) 544.
[5] M. Konuma, Film Deposition by Plasma Techniques, Springer-Verlag, Berlin, 1992.
[6] A. Tissier, J. Khallaayoune, A. Gerodolle, B. Huizing, J. Physique IV 1 (1991) C2–437.
[7] J.-W. He, C.-D. Bai, K.W. Xu, N.-S. Hu, Surf. Coat. Technol. 74–75 (1995) 387.
[8] K.-S. Kim, M. Ikegawa, Plasma Sources Sci. Technol. 5 (1996) 311.
[9] W.L. Morgan, Plasma Chem. Plasma Proc. 12 (1992) 477.
[10] R. Nagpal and A. Garscadden, in: L.G. Christophorou and D.R. James (Eds.), Gaseous Dielectrics VII, Plenum Press, New York, 1994, p. 39; J. Perrin, O. Lervy and M.C. Bordage, Contr. Plasma Phys. 36 (1996) 3.
[11] P. Kac-Nune, J. Perrin, J. Guillon, J. Jolly, Plasma Sources Sci. Technol. 4 (1994) 250.
[12] K. Kameta, M. Ukai, R. Chiba, K. Nagano, N. Kouchi, Y. Hatano and K. Tanaaka, J. Chem. Phys. 95 (1991) 6188; J. Berkovitz, J.P. Greene and H. Cho, J. Chem. Phys., 86 (1987) 1235.
[13] J.W. Gallagher, C.E. Brion, J.A.R. Samson, P.W. Langhoff, J. Phys. Chem. Ref. Data 17 (1988) 9.
[14] R.D.Johnson III, , B.P. Tsai, J.W. Hudgens, J. Chem. Phys. 91 (1989) 3340.
[15] H. Chatham, D. Hils, R. Robertson, A. Gallagher, J. Chem. Phys. 91 (1984) 1770.
[16] E. Krishnakumar, S.K. Srivastava, Contrib. Plasma Phys. 35 (1995) 395.
[17] P. Haaland, Chem. Phys. Lett. 170 (1990) 146.
[18] V. Tarnovsky, H. Deutsch, K. Becker, J. Chem. Phys. 105 (1996) 6315.
[19] J.P. Morrison, J.C. Traeger, Int. J. Mass Spectrom. Ion Phys. 11 (1973) 289.
[20] Y.-K. Kim, M.E. Rudd, Phys. Rev. A 50 (1994) 3954.
[21] H. Deutsch, T.D. Märk, V. Tarnovsky, K. Becker, C. Cornelissen, L. Cespiva, V. Bonacic-Koutecky, Int. J. Mass Spectrom. Ion Proc. 137 (1994) 77.
[22] V. Tarnovsky, A. Levin, K. Becker, R. Basner, M. Schmidt, Int. J. Mass Spectrom. Ion Proc. 133 (1994) 175.
[23] R. Basner, M. Schmidt, V. Tarnovsky, A. Levin, K. Becker, J. Chem. Phys. 103 (1995) 211.
[24] R. Basner, M. Schmidt, H. Deutsch, Contrib. Plasma Phys. 35 (1995) 375.
[25] R. Basner, R. Foest, M. Schmidt, F. Sigeneger, P. Kurunczi, K. Becker, H. Deutsch, Int. J. Mass Spectrom. Ion Phys. 153 (1996) 65.
[26] D. Rapp, P. Englander-Golden, J. Chem. Phys. 43 (1965) 5.
[27] K. Stephan, H. Helm, T.D. Märk, J. Chem. Phys. 73 (1980) 3763.
[28] K. Leiter, P. Scheier, G. Walder, T.D. Märk, Int. J. Mass Spectrom. Ion Proc. 87 (1989) 209.
[29] D. Margreiter, G. Waldner, H. Deutsch, H.U. Poll, C. Winkler, K. Stephan, T.D. Märk, Int. J. Mass. Spectrom. Ion Proc. 100 (1990) 143.
[30] H.U. Poll, C. Winkler, V. Grill, D. Margreiter, T.D. Märk, Int. J. Mass. Spectrom. Ion Proc. 112 (1992) 1.
[31] SIMION, Version 5.0, Idaho National Engineering Laboratory, EG&E Idaho Inc., Idaho Falls, ID, 1992.
[32] R. Basner, R. Foest, M. Schmidt, F. Sigenegger, P. Kurunczi, K. Becker, H. Deutsch, Int. J. Mass Spectrom. Ion Proc. 153 (1996) 65.
[33] V. Grill, G. Walder, D. Margreiter, T. Rauth, H.U. Poll, P. Scheier, T.D. Märk, Z. Phys. D 25 (1995) 217.
[34] Eight Peak Index of Mass Spectra, 2nd ed., Mass Spectrometry Data Center, Aldermaston, 1974; NIST/EPA/NIH Mass Spectral Data Base, V4/5; Chemical Concepts, P.O. Box 100 202, D-62442 Weinheim, Germany, 1994.
[35] G. Cooper, T. Ibuki, C.E. Brion, Chem. Phys. 140 (1980) 133.
[36] K. Leiter, K. Stephan, E. Märk, T.D. Märk, Plasma Chem. Plasma Proc. 4 (1984) 235.

[37] K. Stephan, H. Deutsch, T.D. Märk, J. Chem. Phys. 83 (1985) 5712.
[38] J. Perrin, J.F.M. Aarts, Chem. Phys. 80 (1983) 351.
[39] A.A. Radzig, B.M. Smirnov, Reference Data on Atoms, Molecules and Ions, J.P. Toennies (Ed.), Springer Series in Chemical Physics 31, Springer-Verlag, Berlin–Heidelberg, New York, 1985, p. 376.
[40] Hollemann-Wiberg, Lehrbuch der Anorganischen Chemie, 91–100 ed., de Gruyter Verlag, Berlin–New York, 1985.
[41] L.J. Kieffer, G.H. Dunn, Phys. Rev. 158 (1967) 61.
[42] R.J. Van Brunt, L.J. Kieffer, Phys. Rev. A 2 (1970) 1293.
[43] S. Tsumbuchi, O. Buturi, Appl. Phys. 59 (1990) 808.
[44] T. Tsuboi, K. Nakashima, T. Okawa, Bull. Chem. Soc. Jpn. 64 (1991) 1.
[45] J. Perrin, J.P.M. Schmidt, G. de Rosny, B. Drevillon, J. Huc, A. Loret, Chem. Phys. 73 (1982) 383.
[46] M.A. Ali, Y.-K. Kim, H. Hwang, N.M. Weinberger, M.E. Rudd, J. Chem. Phys. 106 (1997) 9602.